Starch Biocatalyst Based on α-Amylase-Mg/Al-Layered Double Hydroxide Nanohybrids

Felipe Bruna,*,[†] Marita G. Pereira,[‡] Maria de Lourdes T. M. Polizeli,[‡] and João B. Valim[†]

[†]Departamento de Química, Faculdade de Filosofia, Ciências e Letras de Ribeirão Preto and [‡]Departamento de Biologia, Faculdade de Filosofia, Ciências e Letras de Ribeirão Preto, Universidade de São Paulo, Avenida Bandeirantes 3900, Monte Alegre, 14.040-901 Ribeirão Preto, São Paulo, Brazil

S *Supporting Information*

ABSTRACT: The design of new biocatalysts through the immobilization of enzymes, improving their stability and reuse, plays a major role in the development of sustainable methodologies toward the so-called green chemistry. In this work, α-amylase (AAM) biocatalyst based on Mg_3Al-layered double-hydroxide (LDH) matrix was successfully developed with the adsorption method. The adsorption process was studied and optimized as a function of time and enzyme concentration. The biocatalyst was characterized, and the mechanism of interaction between AAM and LDH, as well as the immobilization effects on the catalytic activity, was elucidated. The adsorption process was fast and irreversible, thus yielding a stable biohybrid material. The immobilized AAM partially retained its enzymatic activity, and the biocatalyst rapidly hydrolyzed starch in an aqueous solution with enhanced efficiency at intermediate loading values of ca. 50 mg/g of AAM/LDH. Multiple attachments through electrostatic interactions affected the conformation of the immobilized enzyme on the LDH surface. The biocatalyst was successfully stored in its dry form, retaining 100% of its catalytic activity. The results reveal the potential usefulness of a LDH compound as a support of α-amylase for the hydrolysis of starch that may be applied in industrial and pharmaceutical processes as a simple, environmentally friendly, and low-cost biocatalyst.

KEYWORDS: enzyme immobilization, α-amylase, layered double hydroxides, biohybrid materials, starch converting, adsorption, biomolecules, hydrotalcites
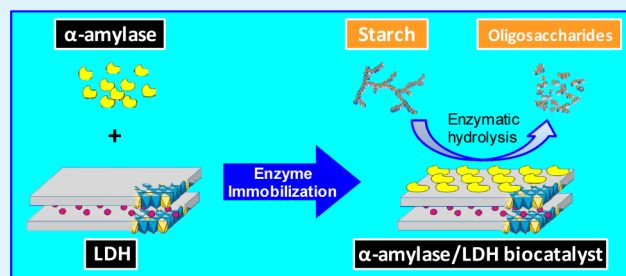
1. INTRODUCTION

Starch is a natural source of chemical energy with a great ubiquity, accessibility, and low cost, which is found in different organs of plants such as seeds, tubers, and fruits. Besides being a staple foodstuff in the human diet since the dawn of civilization, starch is also used as a renewable raw material for several applications such as the production of sweeteners or a source of bioethanol after its treatment.[1] In recent decades, the chemical hydrolysis of starch is being replaced by more advantageous and cleaner biocatalytic processes using starch-converting enzymes such as α-amylases (endo-1,4,α-D-glucan glucohydrolase, EC 3.2.1.1). Those enzymes belong to the family Glycosyl Hydrolase (GH) 13, the major glycoside hydrolase family acting on substrates containing α-glucoside linkages.[2] Such a type of enzyme catalyzes the hydrolysis of internal 1,4-α-D-glycosidic linkages between adjacent glucose units in the linear amylose chain of starch and related polysaccharide polymers leading to the formation of linear and branched oligosaccharides.[3] Moreover, α-amylases are one of the most widely used with approximately 25−33% of the world market enzymes, applied in various areas such as biotechnology, pharmacology, analytical chemistry, food, and textile industry.[4,5]

However, the more widespread industrial and pharmacological applications of these enzymes are hampered by the general lack of low-cost technology to overcome the restricted conditions of free enzyme applications. Therefore, there is a continuing demand for new biotechnologies to improve the stability of these biomolecules and thus meet the requirements set by specific applications. In this context, a promising strategy is to produce enzymes immobilized onto suitable materials which provide several advantages regarding the counterpart enzyme, including repeated or continuous use, enhancement in control of the catalytic process, and easy recovery of enzyme and products with no enzyme contamination. These biomaterials designed are attractive for food, industrial, and pharmaceutical applications.

The immobilization of amylases has become a topic of great interest and been reported for the hydrolysis of starch and the production of maltose. Natural organic polymeric supports such as alginate, chitosan, and cellulose and synthetic organic polymers such as Amberlite, DEAE cellulose, polyesters beads, and activated organic supports containing epoxide

groups are the most widely studied materials.[6−10] However, some drawbacks in using organic matrices, such as low stability to microbiological attack, low robustness to high temperature or organic solvents, and disposal issues, can be solved with the use of inorganic supports. Some inorganic supports such as clays, alumina, and silica, which provide the best features of chemical and physical stability, high biocompatibility, and inertness, have been studied for the immobilization of α-amylases.[11−13] In this context, layered double hydroxides (LDH), also referred to as anionic clays, display unique anionic exchange properties, high structural and compositional versatility, nanosized particle, and low cost. LDH compounds are brucite-like layered materials with a general formula $[M_{1−x}^{II}M_x^{III}(OH)_2]^{x+}X_{x/n}^{n−}\cdot mH_2O$, where M^{II} and M^{III} are divalent and trivalent cations, respectively, and $X^{n−}$ is the interlayer anion, which balances the positive charge originated by the presence of M^{III} in the layers. The layer charge is determined by the M^{II}/M^{III} ratio and can vary $0.20 \leq x \leq 0.33$.[14] Their properties make them very suitable materials for the immobilization of enzymes, which often exhibit an overall negative charge, providing an added value to the immobilized enzymes.[15−20] Among these materials, those consisting in carbonate-intercalated Mg/Al-LDH exhibit greater biocompatibility and are friendlier to the environment and easier to synthesize in the laboratory, becoming outstanding and low-cost nanomaterials.

Bearing in mind that the final use of the immobilized enzyme will be as an industrial biocatalyst, the desirable immobilization process should be simple and robust, avoiding the use of hazardous or unstable reagents, low cost, etc. On this basis, enzyme adsorption onto a solid surface is a well-known phenomenon widely used for immobilizing (or heterogenizing) enzymes.[21,22] This is one of the simplest and cheapest ways to prepare immobilized enzymes, involving weak interactions which are generally less disruptive to the protein structure, usually using no reagents and only a minimum of immobilization steps.[7] Moreover, immobilization generally occurs in the outer surface of the solids, thus reducing the diffusion limitations of bulky substrates for the enzymes immobilized. To date, there has been no published information on the potential usefulness of LDH compounds as supports of α-amylases for the hydrolysis of starch to low molecular weight carbohydrates. In this context, this paper proposes a rational approach to the development of amylase-immobilized biocatalysts with optimized features using LDH compounds as carriers. All steps involved in the design have been herein described. The carrier consisting of Mg/Al (3:1) LDH or hydrotalcite, intercalated with carbonate anions, was prepared and characterized. Next, the process of immobilization through adsorption was optimized. For this purpose, both the effect of contact time and the adsorption−desorption isotherms were studied by means of two different parameters, the amount of protein, and α-amylase units adsorbed. Last, the effect of immobilization in the α-amylase and the efficiency of the biocatalysts for hydrolyzing starch were assessed.

2. EXPERIMENTAL SECTION

2.1. Reagents. The commercial α-amylase preparation (AAM), EC 3.2.1.1 from *Aspergillus oryzae*, was obtained from Sigma-Aldrich in powder form. Bovine serum albumin (BSA) was supplied in lyophilized powder form by Sigma-Aldrich with purity at ≥98%. Bradford reagent was Bio-Rad. Soluble starch was supplied by Reagen (Ultrapure chemicals from Brazil, Inc.). The other chemicals were of analytical grade or better and used as received without further purification.

2.2. Instrumentation. Elemental chemical analysis for Mg and Al were carried out with atomic absorption spectrometry on a high-resolution continuum source atomic absorption spectrometer, model contrAA 700 (Analytik Jena, Jena, Germany). XRD patterns of powder samples were recorded at room temperature under air conditions on a Siemens D-5005 diffractometer using a Cu Kα irradiation source. Scanning electron micrographs (SEM) were recorded with a Zeiss EVO 50 microscope at 20 kV (Carl Zeiss SMT Ltd., U.K.). The surface area values of the LDH were obtained from the N_2 adsorption−desorption measurements, performed at 77 K using a Micromeritics ASAP 2000 analyzer and the Barrett−Emmett−Teller (BET) isotherms. TG curves were obtained using a TA Instruments (USA) SDT 2960 (simultaneous TGA-DTA).

The FT-IR spectrum was obtained through the KBr disc technique on a Shimadzu spectrometer (model IR-prestige 21) in the region of 4000−400 cm^{-1}. One hundred scans were averaged to improve the signal-to-noise ratio at a nominal resolution of 2 cm^{-1}. Zeta potential (ζ-potential) and hydrodynamic diameter (d, nm) were calculated for LDH and for the biocatalyst by electrophoretic light scattering (ELS) and dynamic light scattering (DLS), respectively, using a Zetasizer Nano ZS instrument (Malvern Instruments), with an automatic titration unit (MPT-2). The measurements were performed under the same conditions as the enzyme immobilization using buffered samples of suspensions containing 0.1 M Tris-HCl, pH 7.5 (see below).

Fluorescence spectra of the free and immobilized AAM were recorded at room temperature on a Jobin Yvon Spex Triax 550 Fluorolog III spectrofluorometer. Lamp intensity and photomultiplier sensitivity were corrected for all spectra at the monitored range of wavelengths using the software of the equipment.

2.3. Procedures. *2.3.1. Preparation of the MgAl−CO₃−LDH.* The carbonate-intercalated compound MgAl−CO₃−LDH with a 3:1 M^{II}/M^{III} molar ratio was prepared through the coprecipitation method.[23] Briefly, an aqueous solution (200 mL) containing 0.3 mol of $Mg(NO_3)_2\cdot6H_2O$ and 0.1 mol of $Al(NO_3)_3\cdot9H_2O$ was added slowly, dropwise, to an alkaline solution (500 mL) containing 0.8 mol of NaOH and 0.1 mol of Na_2CO_3. The suspension obtained was hydrothermally treated at 80 °C for 24 h, and the precipitate was washed with distilled water and dried at 60 °C.

2.3.2. Electrophoresis, Protein Determination, and Enzyme Activity Assay. The homogeneity of the commercial enzyme preparation was monitored with sodium dodecyl sulfate−polyacrylamide gel electrophoresis (SDS−PAGE). SDS−PAGE was performed in 8% (w/v) polyacrylamide gel according to the method of Laemli.[24] The molecular weight markers such as protein standard ranging between 15 and 250 kDa were obtained from BioRad (USA).

Protein content in adsorption supernatants was estimated by the method of Bradford.[25] Bio-Rad protein dye reagent concentrate and bovine serum albumin (BSA) as the protein standard were used. Determination of protein adsorbed on biohybrid materials was also quantified directly (direct method) from the Bradford method. Previously, the AAM/LDH biohybrid was completely dissolved using a solution of concentrated phosphoric acid.

Alpha-amylase activity was determined by measuring the reducing sugars by adsorption (glucose equivalents), produced by the hydrolysis of starch, using 3,5-dinitrosalicylic acid (DNS) as described by Miller.[26] A volume of 150 μL of 1.0% soluble starch substrate, in 0.1 M sodium acetate buffer, pH 5.5, was equilibrated in a dry bath heater at 50 °C. The reaction was started by adding 50 μL of a solution containing AAM at the equilibrated substrate stirred at 450 rpm. For the determination of the amylolytic activity from the AAM/LDH biohybrids, the supernatants were immediately separated by centrifugation at 10 000 rpm and 15 min after the enzimatic reaction. This process avoids analytical interferences due to the physicochemical interaction between LDH and the 3-amino-5-nitrosalicylic acid (ANS), the reduced form of DNS. Suspensions with the same amounts of LDH without the enzyme were used as control, and no amount of reducing sugars was detected. The catalytic reaction was carried out for 5 min, and the reaction rate was linear in the whole time interval. A

Table 1. Elemental Analysis, Surface Area, Zeta Potential, z-Average Size, and Unit Cell Parameters of the LDH

wt %							unit cell parameters (Å)		
Mg	Al	H_2O^a	proposed formula	S_{BET} (m^2/g)	zeta potential (mV)	z-average size (d, nm)	d_{003}	c'	a
22.0	7.7	16.4	$[Mg_{0.76}Al_{0.24}(OH)_2] (CO_3)_{0.12}\cdot 0.72H_2O$	113^b	28.3 ± 5.0	174 ± 4^c	7.8	23.24	3.06

[a]Interlamellar and physisorbed water. [b]Coefficient of determination (R^2) > 0.999. [c]Standard deviation of the mean value from 3 measurements.

curve of D-glucose (0.2−2 mmol/L) was used as standard. One unit of amylase activity (U) was defined as the amount of enzyme which releases 1 μmol of glucose equivalent per minute under the assay conditions.

2.3.3. Immobilization: Kinetics and Adsorption−Desorption Isotherms. The commercial α-amylase from *Aspergillus oryzae* was immobilized on the MgAl−CO$_3$−LDH with the adsorption method. Enzyme adsorption was studied under different contact times (adsorption kinetics) and enzyme concentrations (adsorption isotherms) at 4 ± 0.5 °C. Duplicate suspensions containing 20 mg of LDH samples and 10 mL of 0.1 M Tris-HCl buffer (pH 7.5) and α-amylase from Sigma with initial concentration (C_i) ranging between 0.5 and 5 g/L were gently shaken at 40 rpm. The initial concentration of the α-amylase preparation in the kinetic experiments was 1 g/L. Initial α-amylase solutions without the LDH compound were also shaken for 24 h and served as controls to account for losses of protein or enzyme activity by processes different from the adsorption to LDH (adsorption to glassware, precipitation, etc.). The suspensions thus obtained were centrifuged at 10 000 rpm for 15 min, washed several times with buffer, and air dried at room temperature.

The amount of immobilized enzyme was determined by direct and indirect methods, measuring both the enzymatic activity and the protein amount in the supernatants and carriers. The solutions from the washings were also tested for protein desorption.

Indirect Method. Immobilization of α-amylase, given by the enzymatic activity and protein content, was estimated from the difference between the initial (C_i) and the equilibrium (C_e) solution concentrations, respectively

$$C_s = \frac{(C_i - C_e)}{m} \cdot V \tag{1}$$

where C_s (mg/g) is the amount of protein adsorbed, or adsorption capacity, at the equilibrium concentration C_e (mg/L), C_i (mg/L) is the initial protein concentration in solution, m is the adsorbent mass (g), and V is the solution volume (L). The adsorption of α-amylase given by units of enzyme activity can be defined in an analogous way, where C_s is the amount of α-amylase units adsorbed (U/g) at the equilibrium concentration C_e (U/L), C_i is the initial enzymatic activity in solution (U/L), and m (g) and V (L) are the adsorbent mass and solution volume, respectively.

Direct Method. Enzyme activity and protein content were directly quantified from the AAM/LDH biohybrid compound as described above.

Desorption isotherms were obtained immediately after adsorption with the dilution method using samples at *plateau* and intermediate equilibrium points of the isotherm. A volume of 5 mL of the adsorption supernatant was replaced by a buffered solution, performed in the same conditions of the adsorption isotherm experiments, shaken at 4 °C for 24 h, and centrifuged (10 000 rpm, 15 min). Afterward, the protein content in the supernatants was determined. This desorption procedure was repeated four times in duplicate.

Adsorption−desorption results were fitted to the linear form of Freundlich's equation, $C_s = K_f C_e^{Nf}$, and Langmuir−Freundlich's equation, $C_s = (C_m\ C_e^{\ nlf})/(K_d + C_e^{\ nlf})$, where K_f ($mg^{1-Nf}\cdot L^{Nf}\cdot g^{-1}$ or $U^{1-Nf}\cdot mL^{Nf}\cdot mg^{-1}$) and N_f (unitless) are Freundlich's constants, C_m (mg/g or U/mg) is the maximum adsorption capacity, K_d (mg/L or U/mL) is the apparent dissociation constant that includes contributions from binding proteins, and n_{lf} (unitless) is Langmuir−Freundlich's coefficient related to the adsorption cooperativity. Both models were fitted to the experimental data using the Levenberg−Marquardt's nonlinear least-squares method.

In order to reduce and detect diffusional restrictions, buffered suspensions of 0.1 M Tris-HCl, pH 7.5, and containing 5 g/L of the biohybrids were kept under vigorous stirring. The catalytic activity of aliquots, withdrawn every 10 min, was assayed to ensure a constant value.

2.3.4. Stability of the Immobilized AAM: Drying Tolerance of Enzyme Activity. The influence of the drying process in the stability of the immobilized enzyme was evaluated according to the procedure described above. Triplicate 100 μL samples of AAM/LDH suspension containing ca. 1.3 mg of LDH saturated with the enzyme were dried by several procedures: (a) air dried at room temperature, 40 ± 3 and 60 ± 3 °C, (b) dried in a rotational vacuum concentrator (CHRIST, model RVC 2−25 CD plus) at 25, 40, and 60 °C, and (c) freeze dried. The drying time was determined by monitoring the change in weight of the hybrid (W_{hybrid}) versus time (min), and the process was stopped when this parameter remained unchanged, i.e., $dW_{hybrid}/dt = 0$. Then the enzymatic activity of the rehydrated AAM/LDH biohybrids was quantified and compared with the catalytic activity of the undried one.

3. RESULTS AND DISCUSSION

3.1. Characterization of the Support (LDH) and the Enzyme Preparation (AAM). The Mg$_3$Al−CO$_3$−LDH was prepared with the coprecipitation method at pH $\geq$ 10 under air atmosphere conditions. Table 1 summarizes the characterization results of the LDH sample. The proposed formula for Mg$_3$Al−CO$_3$−LDH was obtained from elemental analysis, assuming that all the positive charge is compensated by the maximum possible amount of carbonate anions. A single and well-crystallized LDH phase is obtained for the sample according to its powder XRD analysis with a basal spacing d of 7.8 Å, which is in agreement with that reported previously for carbonate-intercalated MgAl−LDH.[27] The intercalation of carbonate anions in the LDH was confirmed from the PXRD patterns and FT-IR spectra. Physisorbed and interlayer water content were obtained from the TG curves. The surface area was relatively high considering the high structural order of the support but is in agreement with that found in the literature for Mg$_3$Al−CO$_3$−LDH.[28]

The commercial preparation of α-amylase from *A. oryzae* was characterized. The protein content of the commercial preparation was relatively low, $7.3 \pm 0.1\%$ (w/w), which is common in commercial preparations of enzymes.[29] The initial rate of starch hydrolysis was evaluated by a solution containing 1.5 mg/mL of commercial AAM solution. The activity thus determined was 76.6 ± 1.0 U/mg. Specific activity, calculated as the activity per milligram of protein, was 1052.1 ± 9.8 U/mg of protein contained in the AAM preparation.

The SDS-PAGE showed a major band corresponding to the molecular weight described in the literature for α-amylase from *Aspergillus oryzae* (Figure S1).[30] The hydrodynamic diameter (d, nm) of AAM, calculated by DLS under the immobilization conditions (Tris-HCl 0.1 M buffered solution at pH 7.5), was 4.6 ± 1.1 nm. Electrophoretic measures as a function of the pH provided further information on the AAM characteristics. The ζ potential at the above conditions and isoelectric point (IEP) of the protein in aqueous solution was 15 ± 3 mV and 3.8 ± 0.2, respectively (Figure S2).

3.2. Immobilization of AAM. In agreement with various studies performed, electric charge parameters are key parameters influencing on the adsorption capacity of protein in inorganic materials. In this case, the adsorption experiments were carried out at pH 7.5 in buffered solutions, considering the IEP of α-amylase preparation from *A. oryzae*, IEP ca. 3.8 ± 0.2, obtained from the ζ-potential titration curve on water by ELS (Figure S2).[31] Such IEP value is close to those obtained in the literature for α-amylases.[32,33] Thus, the enzyme exhibits a net negative charge at the working pH. Indeed, the ζ potentials of AAM and LDH in 0.1 M of Tris-HCl (pH 7.5) were −15 and +28 mV, respectively. These opposite values should predispose the appearance of electrostatic interactions between AAM and LDH.

Two physicochemical features that define the adsorption process are the equilibrium and kinetics of the adsorption. Their study is the first step toward the understanding and optimization of the immobilization process through adsorption.

3.2.1. Influence of the Contact Time. α-Amylase adsorption onto a solid surface includes several stages. The enzyme in the bulk solution is transported toward the surface through the convection or diffusion processes. Then α-amylase is bound to the solid surface with a defined rate law. A conformational change or rearrangements of the protein which is interacting with the solid is common to occur, even more in the so-called "soft" proteins.[22] Although normally the adsorption process is irreversible, in some cases the detachment from the surface and transport away can occur.

An α-amylase solution was mixed with the LDH to a final load of 0.5 mg of the commercial amylase preparation per milligram of carrier, corresponding to a ratio of 3.6×10^{-2} (w/w) of protein loaded on the LDH at the equilibrium. This value is below the saturation point of the LDH, as it was deduced from the adsorption isotherms (see section 3.2.2). The results depicted in Figure 1 show the kinetic adsorption curve of the α-

amylase on LDH, stated as the percentage of both protein and α-amylase units adsorbed in the supernatants and calculated with the indirect method. Periods of time from 20 min to 26 h were evaluated.

The amount of α-amylase adsorbed on LDH increased sharply with time. Total protein adsorption seems to be directly related to that of the enzymatic activity. More than 90% of the total α-amylase units was adsorbed in 1.5 h, thus indicating a high affinity of AAM for LDH. On the other hand, the enzyme units are faster adsorbed compared to the protein content at first adsorption stages, as it is highlighted by the inset of the Figure 1. This suggests that AAM displayed a faster initial adsorption rate compared with other proteins present in the preparation, which were not previously identified by SDS-PAGE probably due to their lower content in the enzyme preparation. After 8 h of contact time, the amount of adsorbed protein attains a constant value of ∼98% of the C_i at the equilibrium (C_e). Then the adsorption rate, dC_s/dt, was initially higher and decreased with the increase of the elapsed time. Oscillations and local overshoots phenomena in the adsorption kinetic were observed before the saturation was reached (Figure 1, inset). This effect was reproduced by both parameters, α-amylase units and protein adsorbed, with SD less than 5% excluding experimental artifacts. Several authors reported a similar behavior in the adsorption of proteins on solid surfaces of different nature, suggesting orientational and conformational changes of the protein during the adsorption process.[34−37] Overshoot occurs when the adsorption rate is high compared to the transition rate of the protein rearrangement.

Although the overall adsorption process is relatively fast, 24 h of contact time was considered to ensure that the equilibrium was reached between the solution and the aqueous phase.

Knowledge of the kinetic parameters, which is helpful for the prediction of adsorption time, is required for designing and modeling the adsorption process. Two kinetic models widely used in the literature are the Lagergren pseudo-first-order model,[38] which is probably the earliest kinetic model in liquid-phase systems, and the Ho's pseudo-second-order kinetic model.[39] The linearized pseudo-first-order equation may be represented by the following equation

$$\ln(C_s - C_t) = \ln(C_s) - k_1 t \qquad (3)$$

where k_1 (min^{-1}) is the first-order rate coefficient and C_s and C_t (mg/g or U/g) are the adsorption capacities of protein amount or activity units at equilibrium and time t (min), respectively.

The pseudo-second-order model has the advantage that it is not necessary to previously assign an adsorption capacity (C_s) and that it reveals the initial adsorption rate (h) and the constant rate of second order. The pseudo-second-order equation can be represented by the equation

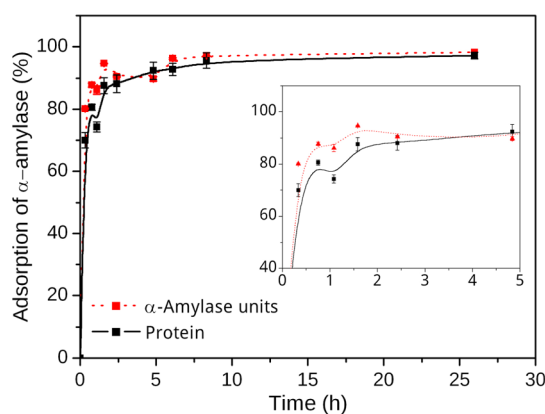$$\frac{t}{C_t} = \frac{1}{k_2 C_s} + \frac{t}{C_s} \qquad (4)$$

Figure 1. Time evolution of the α-amylase adsorption (%), monitoring both protein and enzyme units adsorbed. (Inset) Detail of the first 5 h of the kinetic curve.

Table 2. Kinetic Parameters for Dynamic Adsorption of α-Amylase at the LDH−Water Interface

adsorption kinetic curves	$C_{s\text{-exp}}$ (mg g^{-1} or U g^{-1})	pseudo-first-order			pseudo-second-order			
		$C_{s\text{-calcd}}$ (mg g^{-1} or U g^{-1})	k_1 (h^{-1})	R^2	$C_{s\text{-calcd}}$ (mg g^{-1} or U g^{-1})	k_2 (× 10^3) (g mg^{-1} min^{-1} or g U^{-1} min^{-1})	h (mg g^{-1} min^{-1} or U g^{-1} min^{-1})	R^2
protein	36.2 ± 0.5	9.28−3.84	0.31 ± 0.11	0.56	36.7 ± 0.3	2.9 ± 0.9	3.86 ± 1.26	0.99
AAM units	63.2 ± 0.1	12.55−6.75	0.29 ± 0.07	0.71	63.3 ± 0.4	2.1 ± 0.7	8.47 ± 4.51	0.99

where k_2 (g mg^{-1} min^{-1} or g U^{-1} min^{-1}) is the second-order rate coefficient for the enzyme adsorption given by mass of protein or α-amylase units, respectively. The second-order rate constants (h) were used to calculate the initial adsorption rate given by

$$h = k_2 C_s^2 \qquad (5)$$

The results of the adsorption kinetics were fitted to the models described above (Figure S3). The first-order rate constants, second-order rate constants, and calculated initial adsorption rate values are shown in Table 2. It was observed that neither for the α-amylase units nor for the protein adsorption does the pseudo-first-order model properly fit the experimental data, according to the coefficient of determination (R^2). Thus, the Lagergren model was not appropriate to describe the entire adsorption process of AAM onto LDH. Probably, it is due to its intricate adsorption process, where more than one adsorption step occurs. However, kinetic modeling of AAM adsorption onto LDH followed a pseudo-second-order model, which is based on the assumption that the rate-limiting step in the adsorption process may be chemisorption. The C_s values calculated ($C_{s\text{-calcd}}$) were in agreement with the experimental values ($C_{s\text{-exp}}$) for both kinetic curves, and a coefficient of determination value $R^2 > 0.99$ shows that the model can be applied for the entire adsorption process. Similar results were found by Jin and co-workers for the adsorption of hemoglobin onto gold nanoparticles supported by a MgAl−LDH, whose adsorption kinetic curves fitted better to the pseudo-second-order model.[40]

3.2.2. Adsorption−Desorption Isotherms. Adsorption isotherms of α-amylase from *A. oryzae* (Sigma) on the LDH sample were determined by monitoring both the protein and the α-amylase units adsorbed (Figure 2A). The AAM adsorption increases with the AAM concentration in the solution. AAM is almost completely adsorbed in diluted solutions, reaching up to 97% for both protein and α-amylase units adsorbed from the supernatants in solutions with $C_i < 1.5$ g/L of AAM (Figure 2C).

The shape of the experimental data is quite similar to the Langmuir isotherm. This is because researchers used the theory/Langmuir model of general affinity interaction typically as a first approach for the analysis of the protein adsorption behavior (Figure S4). However, some complexities that may influence the protein adsorption process, such as multiple-site binding, heterogeneous nature of the surface, and cooperative interactions, can result in the misapplication of the Langmuir model to a Langmuir-looking protein adsorption isotherm.[21,41] In order to achieve a more suitable description of the enzyme adsorption on LDH, we proposed to use other models such as (a) the Freundlich model, which comprises the heterogeneity of the adsorbent surface, and (b) the composite Langmuir−Freundlich model, a two-parametric model able to explain cooperativity and binding heterogeneity in quantitative terms.

Accordingly, the adsorption parameters of AAM on LDH were obtained by the nonlinear fitting of the adsorption isotherms to the Freundlich and the Langmuir−Freundlich equations (Table 3). Adsorption isotherms and parameters, K_f and K_d, indicated a high affinity of the protein for the LDH. Both the amount of protein and the α-amylase units showed the same adsorption profile, displaying H-type adsorption isotherms ("high affinity") according to the classification reported by Giles et al. (1960).[42] These types of isotherms involve strong interactions between the adsorbent and the
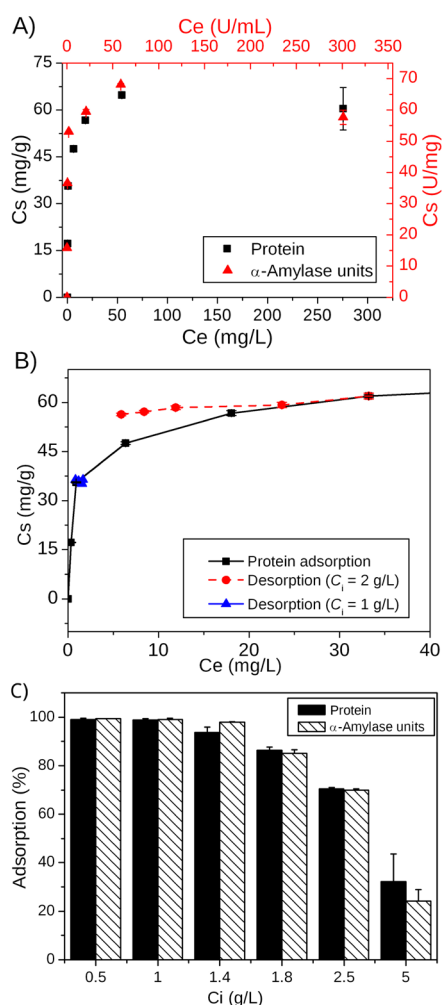

Figure 2. (A) Adsorption and (B) desorption isotherms of α-amylase on LDH. (C) Percentage of protein and α-amylase units adsorbed for each initial concentration (C_i) of the adsorption isotherm.

protein that could be attributed to electrostatic or Coulomb interactions, considering the opposite charge values obtained for AAM and LDH in the buffered solutions at pH 7.5. These adsorption isotherms are typical of systems with bulky solutes like polymeric species or adsorption of micelles.

The Langmuir−Freundlich model was better suitable for describing the overall adsorption behavior, showing C_m values close to the experimental data. It is noteworthy that the Langmuir−Freundlich coefficient n_{fl} shows different values, although they apparently presented similar isotherm profiles. For the protein isotherm, related to the total protein content, $n_{fl} < 1$ suggested a negative cooperativity in the adsorption process. However, for the enzyme activity, which is a more specific and sensitive method for the detection of the α-amylase, N_f values closer to 0 and $n_{fl} > 1$ suggested a heterogeneous nature of protein adsorption and positive cooperativity in binding. Therefore, the positive cooperativity found in the enzymatic activity results may indicate that the overall adsorption process of AAM is favored by attractive forces, due to lateral enzyme−enzyme interactions. Meanwhile, the negative cooperativity in the protein adsorption may indicate that AAM adsorbed hinders the adsorption of other proteins in the solution, which adversely compete for the LDH adsorption sites.[21]

Table 3. Freundlich and Langmuir–Freundlich Parameters for AAM Adsorption on LDH and Hysteresis Coefficient *H*

adsorption istotherm	Freundlich model			H^a	Langmuir–Freundlich model			
	K_f	N_f	R^2		C_m	K_d	n_{lf}	R^2
protein	34.2 ± 4.3	0.13 ± 0.03	0.92	0.27	66.7 ± 4.6	0.93 ± 0.21	0.66 ± 0.16	0.99
AAM units	38.9 ± 6.1	0.10 ± 0.04	0.82		61.9 ± 2.4	2.75 ± 0.92	1.20 ± 0.27	0.98

$^a H = N_{f\text{-des}}/N_f$; $N_{f\text{-des}}$ calculated from the protein desorption at $C_i = 2$ mg/mL

Figure 2B shows the desorption isotherm of the protein from the adsorption isotherm points corresponding to $C_i = 1$ and 2 g/L of AAM preparation. The desorption curves indicated a high irreversibility of the adsorption process, slightly steeper for AAM concentrations below the saturation of the LDH. This agrees with the high hysteresis found and is depicted by the low H coefficient value (Table 3). Therefore, the results confirmed the high affinity of the protein for the LDH, supporting the hypothesis that the enzyme could be bound to the surface by multiple attachments.[22]

These results are comparable to those obtained by several authors where high irreversibility in the adsorption process of enzymes on LDH was reported. For the immobilization of aminopeptidase on a MgAl–LDH, Frey and co-workers suggested a very strong and irreversible association between the enzyme and the LDH under the conditions tested.[43] Forano and co-workers did not observe an effective enzyme release, except when the biohybrid enzyme/LDH material was stirred in buffered solution.[18] However, Vial and co-workers found a high reversibility of the adsorption process of urease to a ZnAl–LDH which is enhanced by the ionic strength of the solution.[44] This highlights the complexity of the immobilization of biopolymers, which depends on the enzyme/LDH biosystem selected and the experimental conditions, such as pH and ionic strength. In the case of the AAM/LDH biohybrid, the high resistance displayed for AAM to be desorbed from LDH in buffered water is interesting from the point of view of the applicability of these nanomaterials as enzyme supports.

3.3. Effect of Immobilization on Enzyme Activity. The catalytic activity of the AAM/LDH biohybrids, obtained from the different adsorption isotherm points with C_s between 17 and 65 mg/g, was tested for the hydrolysis of starch. The results indicated that the biocatalyst activity increased with the amount of enzyme immobilized, following a slight sigmoid pattern (Figure 3). On the other hand, the efficiency or specific activity of the biocatalyst, defined as the activity units per AAM immobilized (loading), was slightly higher for average values of immobilized enzyme.

Several authors have reported the effects of different coverage of proteins immobilized onto solid surfaces.[21,45,46] At low surface coverage, the enzymes maximize their interaction with the LDH surface, leading to relaxation with some degree of spreading on the LDH surface. This effect leads to an alteration in the native conformation that reduces the catalytic activity. In an intermediate surface coverage, enzyme–enzyme interactions afford the preservation of active enzyme conformation. On the other hand, higher protein loadings ($C_s > 50$ mg/g) may produce some enzyme aggregation on the LDH surface that reduces the mass transfer of substrate molecules to the catalytic sites, suggesting multilayer adsorption of the AAM preparation.

From the results obtained in the adsorption kinetics, more than one type of protein in the commercial preparation of α-amylase was revealed. Therefore, competition among proteins of the AAM preparation for the adsorption sites may take place at values of $C_i > 1.5$ g/L, where the protein amount was not
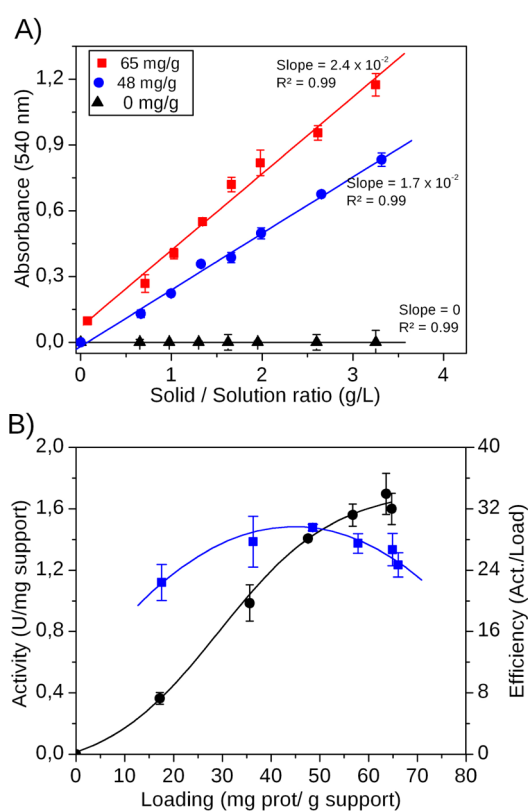

Figure 3. (A) Hydrolysis of starch for increasing amounts of LDH and biohybrids corresponding to loadings $C_s = 0$, 48, and 65 mg AAM/g LDH (black triangles, blue circles, and red squares, respectively). (B) Effect of α-amylase loading on the enzyme activity (black circles) and efficiency (blue squares).

totally adsorbed in the adsorption equilibrium (Figure 2C). This may also justify the decreased efficiency of the biocatalyst at higher loading values. However, a similar amount of α-amylase units and protein was adsorbed at the equilibrium for the whole adsorption isotherm. This result suggests that enzyme competition effects were not meaningful. This is probably due to the low proportion of other proteins different from α-amylase in the enzyme preparation, as the SDS-PAGE inferred.

The activity of the free enzyme was also compared with the final activity found for the immobilized α-amylase. The enzymatic activity was partially retained in all cases, showing a decrease in the activity of the AAM bound to LDH up to 40-fold compared to free counterpart. This is a common effect observed in nonspecific adsorption of several enzymes randomly bound to the LDH surface.[15,18,43] Nonetheless, a substantial portion of the immobilized AAM in the AAM/LDH biohybrid remains active and catalyzes the rapid hydrolysis of starch in a novel multifunctional biomaterial (Figure 3A).

Several hypotheses were considered in order to confirm the causes of the general decrease observed in the final enzyme
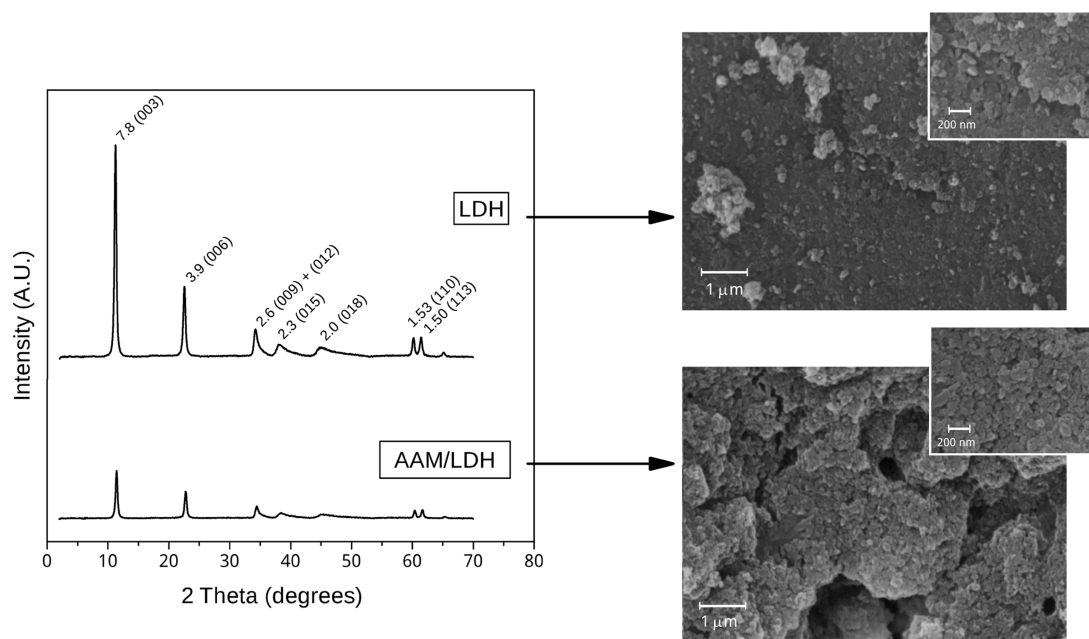
Figure 4. PXRD patterns (left) and SEM micrographs (right) of LDH (top) and AAM/LDH (bottom, C_s = 65 mg/g).

activity once AAM is immobilized on the LDH: (a) distortions of the tertiary structure of the immobilized protein, (b) protein desorption by washing with Tris-HCl buffer after immobilization, (c) formation of enzyme aggregates and diffusional restrictions, (d) structural disturbance of the protein caused by the drying process, and (e) enzyme inhibition by the LDH constituents from its partial dissolution. Although there are various scenarios that could justify the decrease of the enzyme activity in systems with LDH, there are few studies that address all the aspects mentioned.

3.3.1. Interaction with the Support: Characterization of the AAM/LDH Biomaterial. Structural and morphological characterization of the AAM immobilized onto LDH compound was performed.

Powder X-ray Diffraction (PXRD). XRD patterns of AAM/LDH (Figure 4), showing a basal space of d_{003} = 0.77 nm, were typical of those widely reported hydrotalcite compounds intercalated with carbonate anions.[27] The sharp peaks provided evidence of a well-crystallized LDH structure of the biocatalyst. However, X-ray diffraction patterns showed a reduction in the intensity of the reflections compared to the pristine LDH and similar basal spacing. This suggests that AAM adsorption occurred mainly on the LDH surface.

Electrophoretic and Dynamic Light Scattering. The zeta potential in a stable colloidal solution containing the AAM/LDH biohybrid at a loading value of C_s = 65 mg/g was determined. The immobilization of AAM to the support caused a severe decrease in the ζ potential from +28 (LDH) to −18 mV (AAM/LDH), achieving values close to those of pure AAM. This shielding effect of the charges of LDH confirms that the AAM immobilization occurred through electrostatic interactions between the enzyme and the support. Moreover, an increase was observed in the hydrodynamic diameter of the biomaterial in suspension (275 ± 5 nm) compared to that of the pristine LDH (174 ± 4 nm).

Scanning Electron Micrographs. The SEM images, included in Figure 4, showed that the LDH sample consisted of small crystals with the usual densely packed texture of LDH

compounds intercalated with inorganic anions such as CO_3^{2-}, SO_4^{2-}, or NO_3^{-}. However, biomolecule adsorption on the solid surface produces a noticeable change in its morphology, showing a cracked and ill-defined shape of thinner particles.[15,47] This modification of the LDH morphology favors the diffusion of the substrate toward the adsorbed enzyme, which is in agreement with the results observed in Figure 3A.

Fluorescence Spectroscopy. Figure 5 shows the fluorescence spectra of the AAM/LDH biohybrid in colloidal aqueous
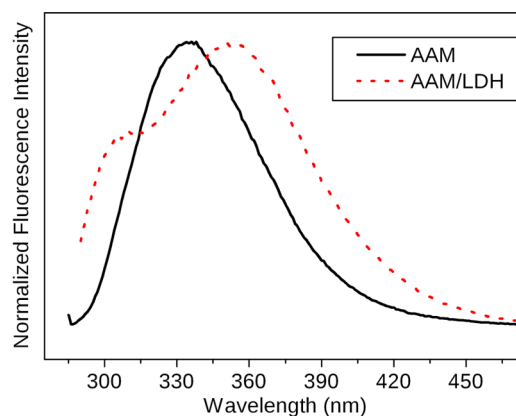

Figure 5. Fluorescence emission spectra of free AAM (black line) and the colloidal suspension of AAM/LDH biohybrid (red dots). Excitation at 270 nm.

suspension upon excitation at 270 nm compared to native enzyme in the same experimental conditions. The fluorescence emission spectrum of AAM/LDH confirmed the immobilization of AAM on the support. The tryptophan (Trp) units in α-amylase of *A. oryzae*, which are buried in the interior of the protein in a less polar environment, fluoresce with a peak close to 335 nm. When the AAM was immobilized, the fluorescence yield decreased and a noticeable red shift of the peak position toward 350 nm was observed with a shoulder centered at 309 nm. These values are close to the maximum emission produced

by both fluorophores, tyrosine and tryptophan, at 305 and 350 nm, respectively. This red shift indicates a conformational change of the AAM, where the tryptophan residues previously buried in the native protein conformation, became more accessible to the solvent molecules.[48,49]

On the other hand, tyrosine (Tyr) fluorescence emission is generally not visible for native conformational states of multitryptophan proteins like α-amylase due to distinct Fröster resonance energy transfer (FRET) from tyrosine to tryptophan.[50] In this regard, more information can be obtained on the structural compactness of the native and unfolded states of proteins, evaluating the fluorescence emission spectra at different excitation wavelengths: 270, 280, and 290 nm (Figure 6). At excitation wavelengths between 270 and 280 nm, both
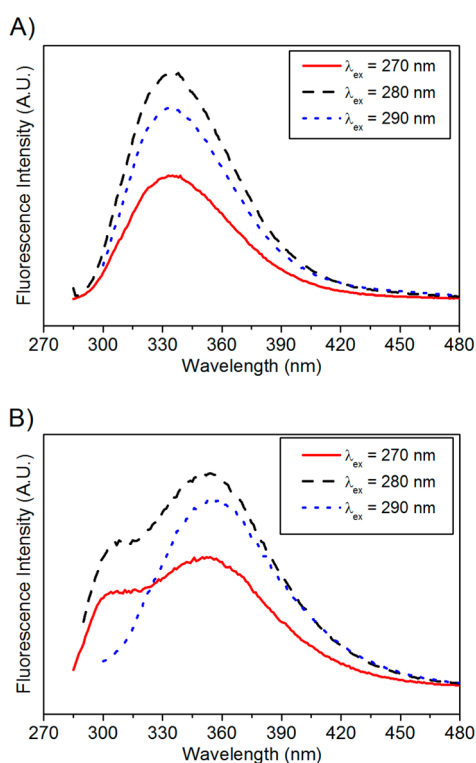

Figure 6. Fluorescence emission spectra of (A) AAM and (B) AAM/LDH obtained with different excitation wavelengths: λ_{exc} = 270 (red solid line), 280 (black dashed line), and 290 nm (blue dot line).

tyrosine and tryptophan fluoresce, while at 290 nm only tryptophan fluoresces. Emission spectra of native AAM are very similar and represent Trp emission either because only Trp was excited at 290 nm or because Tyr excitation at 270−280 nm leads to FRET effects (Figure 6A). However, in the case of the immobilized enzyme, different emission spectra were observed depending on the excitation wavelength (Figure 6B). This reduction of FRET in the immobilized enzyme, which makes the Tyr fluorescence detectable, confirmed the spreading of the enzyme on LDH.

These conclusions also agree with the discussion detailed in the adsorption kinetics, and they justify the loss of AAM activity when it is immobilized. Similar results were reported by several authors for the immobilization of different proteins on LDH.[15,19,51]

3.3.2. Protein Leakage. Enzyme leakage can occur because the protein is noncovalently bound to the matrix, especially washing with buffered aqueous solutions.[44] Because of this we

considered the possibility of an activity decrease due to some AAM desorption during the washings with Tris-HCl-buffered solutions (pH 7.5). However, supernatants of the washings were assayed, and no significant protein amount or activity was found (data not shown). On the other hand, the content of protein on the biomaterials directly analyzed agreed with that estimated by the indirect method (Figure 7). These results,
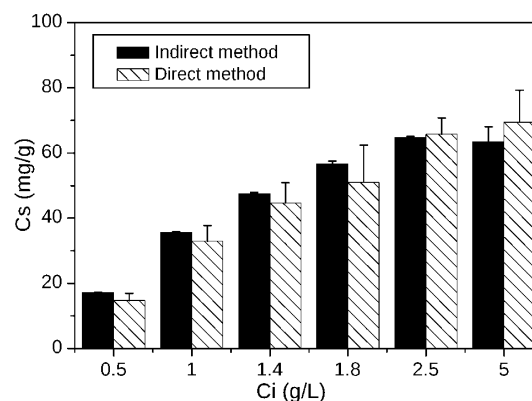

Figure 7. Indirect and direct estimation of the amount of adsorbed protein (C_s) for each initial concentration (C_i) of the adsorption isotherm.

together with the desorption isotherms, confirmed that no significant desorption of AAM occurs after its immobilization. Likewise, they also indicated that there are no significant losses of AAM by any other process different from the adsorption to LDH.

3.3.3. Formation of Enzyme Aggregates and Diffusional Restrictions. According to the results discussed above, enzyme aggregation on the LDH surface is not likely in biohybrids with loading values up to 50 mg/g, which corresponds to C_i = 1.5 g/L (Figure 3). It must also be considered that increased amounts of the biohybrid material in the reaction medium may cause some diffusional restrictions. However, Figure 3A shows that the increase of catalytic activity was directly proportional to the amount of biohybrid added. This suggested that there were no noticeable diffusional limitations of the substrate caused by the increase in the solid/solution ratio in the stirred reaction medium. However, diffusional limitation may occur by the orientation of nonspecific protein immobilized on the solid surface, especially with bulky substrates such as starch.[21]

3.3.4. Influence of the Drying Process on the AAM Activity. Protease activity and reactions such as oxidation, which can initiate protein unfolding, can reduce the lifetime of proteins in solutions. Storage in the dry state of the immobilized proteins offers numerous benefits for increasing the useful life of protein-based materials, preventing enzyme leakage during long-term storage, as well as easier transportation and sample handling. Therefore, different methods, freeze drying, rotational vacuum drying, and air drying, were tested without any stabilizers in order to dry the biocatalysts with minor losses of activity up to dW_{hybrid}/dt = 0. Figure 8 shows the activity of the biocatalyst in aqueous suspension (without drying) compared to the residual activity of the predried and rehydrated AAM/LDH biohybrid.

In the case of the air-drying method, the catalytic activity significantly decreased with the increase in the temperature. However, the residual activity was similar to the control using the rotational vacuum-drying method at the interval of
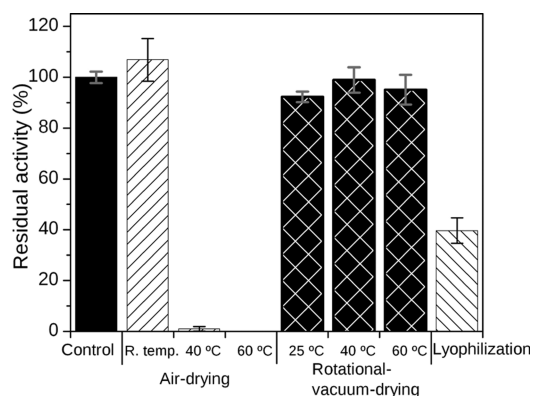
Figure 8. AAM/LDH activity for hydrolyzing starch of the undried biohybrid (control), compared with the residual activity of the rehydrated AAM/LDH sample, previously dried by air drying (at room temperature and 40 and 60 °C), rotational vacuum drying (at 25, 40, and 60 °C), and freeze drying. C_s = 65 mg AAM/g LDH.

temperatures studied. This may be related to the length of time taken for drying the samples. The time required for the air-drying method was 5- and 16-fold higher at 60 and 40 °C, respectively, compared to the time used on rotational vacuum drying. On the other hand, freeze drying caused higher conformational stresses compared with the rotational vacuum-drying and air-drying (at room temperature) methods. These results demonstrated that both the methodology and the conditions used for drying the AAM/LDH biohybrid may cause whole or partial decrease of its catalytic activity. Further studies are needed to better understand the behavior of the AAM/LDH system related to the drying process.

Furthermore, the drying method and the conditions used (air drying at room temperature) did not justify the decrease observed in the catalytic activity of immobilized AAM compared to the free enzyme.

3.3.5. Influence of Ions on the AAM Activity. Partial dissolution of the LDH layers can release its structural ions into the aqueous medium and may affect the catalytic activity of AAM. Table 4 shows that the enzyme activity is not sensitive to magnesium or carbonate at the concentrations tested, corresponding to a partial and total dissolution of the LDH

Table 4. Influence of Ions on the AAM Activity at Different Concentrations Equivalent to the Partial or Total Dissolution of the LDH[a]

compounds	concentration (mM)	equivalent dissolved fraction of LDH (wt %)	relative AAM activity (%)[b]
control (no addition)			100
MgCl₂	1	0.06 (Mg²⁺)	101
	20	1.25 (Mg²⁺)	98
AlCl₃	1	0.20 (Al³⁺)	107
	5	1.00 (Al³⁺)	66
MgCl₂ + AlCl₃	20 + 6 (respectively)	1.25 (Mg²⁺) and 1.20 (Al³⁺)	65
Na₂CO₃	1	0.40 (CO₃²⁻)	106
	2.5	1.00 (CO₃²⁻)	92
CaCO₃	1	0.40 (CO₃²⁻)	96

[a]Samples incubated for 30 min before the reaction. [b]Standard errors < 5%.

amount used in the experiments. However, enzyme activity is affected with high concentrations of aluminum in the solution.

Immobilization conditions in a buffered solution at pH 7.5 are unfavorable for dissolving the LDH layers.[52] According to the results obtained in Figures 1 and 2, no significant inhibition of the unbound enzyme was observed, which would cause an overestimation of the adsorption of α-amylase units compared with the protein adsorbed. However, the AAM/LDH was applied for 5 min at the AAM optimum pH (pH 5.5) for the evaluation of the hydrolysis of starch. The conditions used were considered insufficient to achieve concentrations higher than 1 mM of Al in the solution, which is equivalent to dissolution of 20% of LDH added. Consequently, in these conditions the activity was not significantly influenced by the chemical inhibition of the enzyme.

Higher residence times and more aggressive acidic conditions (pH < 4) would promote gradual weathering of the LDH structure.[53,54] These properties of the LDH compounds have been applied for the slow release of pharmacological or agrochemical active compounds.[55−57] Recently, Zou and Plank demonstrated that the release of a cellulase, previously incorporated in a LDH of Mg/Al, maintains its original conformation with a 92% of activity retention.[58] Similar results were suggested by Bellezza and co-workers for the immobilization of myoglobin (Mb) on LDH.[19] If these findings are extended to the AAM/LDH system, complete dissolution of the biohybrid, and release of AAM probably would produce only a partial inhibition of enzyme activity. Therefore, our research group is currently conducting a comprehensive study toward this aspect.

4. CONCLUSIONS

The biomaterial obtained by the immobilization of AAM on the surface of the inorganic Mg₃Al−CO₃ LDH retained the α-amylase activity and was capable to catalyze the rapid hydrolysis of starch in the solution. This cheap and simple procedure of enzyme immobilization demonstrates that LDH compounds can be used as carriers for a commercial α-amylase preparation. The adsorption of AAM to the LDH was relatively fast. A high and essentially irreversible interaction between AAM and LDH contributed to decrease the mobility of the enzyme preparation, forming a stable biocatalyst and allowing its recovery from the reaction mixture by centrifugation. The nonspecific AAM immobilization occurs by multiple attachments through electrostatic interactions which cause the spreading of the enzyme on the LDH surface. The orientational and conformational change caused by the immobilization partially decreased the amylase activity. The amount of immobilized enzyme is a parameter which must be optimized for improving the performance of the biocatalyst. The biocatalyst was successfully stored in dry state, retaining up to 90% of its initial activity for at least 5 weeks. However, our experiments showed that the drying method and the conditions used must be considered in order to maximize the retention of the amylase activity of the biocatalyst. This study provides the basis for the development of multifunctional biomaterials based on enzymes/LDH with potential applications on industrial processes such as the production of biodiesel or biomedical systematic therapies.

■ ASSOCIATED CONTENT

Ⓢ Supporting Information

The Supporting Information is available free of charge on the ACS Publications website at DOI: 10.1021/acsami.5b05668.

SDS-PAGE of the commercial enzyme preparation, zeta-potential curve of AAM as a function of the pH, kinetic and isotherm models of the AAM adsorption on LDH (PDF)

■ **AUTHOR INFORMATION**

Corresponding Author

*E-mail: fbruna@outlook.com.

Notes

The authors declare no competing financial interest.

■ **REFERENCES**

(1) Röper, H. Renewable Raw Materials in Europe — Industrial Utilisation of Starch and Sugar [1]. *Starch - Stärke* **2002**, *54*, 89−99.

(2) Van der Maarel, M. J. E. C.; van der Veen, B.; Uitdehaag, J. C. M.; Leemhuis, H.; Dijkhuizen, L. Properties and Applications of Starch-Converting Enzymes of the α-Amylase Family. *J. Biotechnol.* **2002**, *94*, 137−155.

(3) Regulapati, R.; Malav, P. N.; Gummadi, S. N. Production of Thermostable α-Amylases by Solid State Fermentation-A Review. *Am. J. Food Technol.* **2007**, *2*, 1−11.

(4) BeMiller, J.; Whistler, R. *Starch. Chemistry and Technology*, 3rd ed; Academic Press: San Diego, 2009.

(5) Gangadharan, D.; Madhavan Nampoothiri, K.; Sivaramakrishnan, S.; Pandey, A. Immobilized Bacterial α-Amylase for Effective Hydrolysis of Raw and Soluble Starch. *Food Res. Int.* **2009**, *42*, 436−442.

(6) Konsoula, Z.; Liakopoulou-Kyriakides, M. Starch Hydrolysis by the Action of an Entrapped in Alginate Capsules α-Amylase from Bacillus Subtilis. *Process Biochem. (Oxford, U. K.)* **2006**, *41*, 343−349.

(7) Datta, S.; Christena, L. R.; Rajaram, Y. R. S. Enzyme Immobilization: An Overview on Techniques and Support Materials. *3 Biotech* **2013**, *3*, 1−9.

(8) Kumari, A.; Kayastha, A. M. Immobilization of Soybean (Glycine Max) α-Amylase onto Chitosan and Amberlite MB-150 Beads: Optimization and Characterization. *J. Mol. Catal. B: Enzym.* **2011**, *69*, 8−14.

(9) Singh, K.; Kayastha, A. M. Optimal Immobilization of α-Amylase from Wheat (Triticum Aestivum) onto DEAE-Cellulose Using Response Surface Methodology and Its Characterization. *J. Mol. Catal. B: Enzym.* **2014**, *104*, 75−81.

(10) Cakmakci, E.; Danis, O.; Demir, S.; Mulazim, Y.; Kahraman, M. V. Alpha-Amylase Immobilization on Epoxy Containing Thiol-Ene Photocurable Materials. *J. Microbiol. Biotechnol.* **2013**, *23*, 205−210.

(11) Reshmi, R.; Sanjay, G.; Sugunan, S. Enhanced Activity and Stability of α-Amylase Immobilized on Alumina. *Catal. Commun.* **2006**, *7*, 460−465.

(12) Sanjay, G.; Sugunan, S. Immobilization of α-Amylase onto K-10 Montmorillonite: Characterization and Comparison of Activity in a Batch and a Fixed-Bed Reactor. *Clay Miner.* **2005**, *40*, 499−510.

(13) Sohrabi, N.; Rasouli, N.; Torkzadeh, M. Enhanced Stability and Catalytic Activity of Immobilized α-Amylase on Modified Fe_3O_4 Nanoparticles. *Chem. Eng. J. (Amsterdam, Neth.)* **2014**, *240*, 426−433.

(14) Cavani, F.; Trifirò, F.; Vaccari, A. Hydrotalcite-Type Anionic Clays: Preparation, Properties and Applications. *Catal. Today* **1991**, *11*, 173−301.

(15) Charradi, K.; Forano, C.; Prevot, V.; Madern, D.; Ben Haj Amara, A.; Mousty, C. Characterization of Hemoglobin Immobilized in MgAl-Layered Double Hydroxides by the Coprecipitation Method. *Langmuir* **2010**, *26*, 9997−10004.

(16) Touisni, N.; Charmantray, F.; Helaine, V.; Forano, C.; Hecquet, L.; Mousty, C. Optimized Immobilization of Transketolase from E. Coli in MgAl-Layered Double Hydroxides. *Colloids Surf., B* **2013**, *112*, 452−459.

(17) Choy, J. H.; Park, M.; Oh, J. M. Bio-Nanohybrids Based on Layered Double Hydroxide. *Curr. Nanosci.* **2006**, *2*, 275−281.

(18) Forano, C.; Vial, S.; Mousty, C. Nanohybrid Enzymes-Layered Double Hydroxides: Potential Applications. *Curr. Nanosci.* **2006**, *2*, 283−294.

(19) Bellezza, F.; Cipiciani, A.; Latterini, L.; Posati, T.; Sassi, P. Structure and Catalytic Behavior of Myoglobin Adsorbed onto Nanosized Hydrotalcites. *Langmuir* **2009**, *25*, 10918−10924.

(20) Rojas, R.; Giacomelli, C. E. Size-Tunable LDH-Protein Hybrids toward the Optimization of Drug Nanocarriers. *J. Mater. Chem. B* **2015**, *3*, 2778−2785.

(21) Rabe, M.; Verdes, D.; Seeger, S. Understanding Protein Adsorption Phenomena at Solid Surfaces. *Adv. Colloid Interface Sci.* **2011**, *162*, 87−106.

(22) Norde, W. My Voyage of Discovery to Proteins in Flatland···and beyond. *Colloids Surf., B* **2008**, *61*, 1−9.

(23) Reichle, W. Synthesis of Anionic Clay Minerals (mixed Metal Hydroxides, Hydrotalcite). *Solid State Ionics* **1986**, *22*, 135−141.

(24) Laemmli, U. K. Cleavage of Structural Proteins during the Assembly of the Head of Bacteriophage T4. *Nature (London, U. K.)* **1970**, *227*, 680−685.

(25) Bradford, M. M. A Rapid and Sensitive Method for the Quantitation of Microgram Quantities of Protein Utilizing the Principle of Protein-Dye Binding. *Anal. Biochem.* **1976**, *72*, 248−254.

(26) Miller, G. L. Use of Dinitrosalicylic Acid Reagent for Determination of Reducing Sugar. *Anal. Chem. (Washington, DC, U. S.)* **1959**, *31*, 426−428.

(27) Chaara, D.; Bruna, F.; Ulibarri, M. A.; Draoui, K.; Barriga, C.; Pavlovic, I. Organo/layered Double Hydroxide Nanohybrids Used to Remove Non Ionic Pesticides. *J. Hazard. Mater.* **2011**, *196*, 350−359.

(28) Crepaldi, E. L.; Tronto, J.; Cardoso, L. P.; Valim, J. B. Sorption of Terephthalate Anions by Calcined and Uncalcined Hydrotalcite-like Compounds. *Colloids Surf., A* **2002**, *211*, 103−114.

(29) Salis, A.; Pinna, M.; Monduzzi, M.; Solinas, V. Comparison Among Immobilised Lipases on Macroporous Polypropylene toward Biodiesel Synthesis. *J. Mol. Catal. B: Enzym.* **2008**, *54*, 19−26.

(30) Takagi, T. Confirmation of Molecular Weight of Aspergillus Oryzae α-Amylase Using the Low Angle Laser Light Scattering Technique in Combination with High Pressure Silica Gel Chromatography. *J. Biochem.* **1981**, *89*, 363−368.

(31) Salgin, S.; Salgin, U.; Bahadir, S. Zeta Potentials and Isoelectric Points of Biomolecules: The Effects of Ion Types and Ionic Strengths. *Int. J. Electrochem. Sci.* **2012**, *7*, 12404−12414.

(32) Sabaté, R.; Estelrich, J. Interaction of α-Amylase with N-Alkylammonium Bromides. *Int. J. Biol. Macromol.* **2001**, *28*, 151−156.

(33) Fischer, E. H.; de Montmollin, R. Propriétés de L'α-Amylase d'Aspergillus Oryzae Cristallisée. Sur Les Enzymes Amylolytiques XIX. *Helv. Chim. Acta* **1951**, *34*, 1994−1999.

(34) Wertz, C. F.; Santore, M. M. Adsorption and Reorientation Kinetics of Lysozyme on Hydrophobic Surfaces. *Langmuir* **2002**, *18*, 1190−1199.

(35) Petrone, L.; Aldred, N.; Emami, K.; Enander, K.; Ederth, T.; Clare, A. S. Chemistry-Specific Surface Adsorption of the Barnacle Settlement-Inducing Protein Complex. *Interface Focus* **2014**, *5*, 1−11.

(36) Roach, P.; Farrar, D.; Perry, C. C. Interpretation of Protein Adsorption: Surface-Induced Conformational Changes. *J. Am. Chem. Soc.* **2005**, *127*, 8168−8173.

(37) Daly, S. M.; Przybycien, T. M.; Tilton, R. D. Coverage-Dependent Orientation of Lysozyme Adsorbed on Silica. *Langmuir* **2003**, *19*, 3848−3857.

(38) Lagergren, S. Y. Zur Theorie der Sogenannten Adsorption Gelöster Stoffe. *K. Sven. Vetenskapsakad. Handl.* **1898**, *24*, 1−39.

(39) Ho, Y. S.; McKay, G. Pseudo-Second Order Model for Sorption Processes. *Process Biochem. (Oxford, U. K.)* **1999**, *34*, 451−465.

(40) Jin, L.; He, D.; Li, Z.; Wei, M. Protein Adsorption on Gold Nanoparticles Supported by a Layered Double Hydroxide. *Mater. Lett.* **2012**, *77*, 67−70.

(41) Latour, R. A. The Langmuir Isotherm: A Commonly Applied but Misleading Approach for the Analysis of Protein Adsorption Behavior. *J. Biomed. Mater. Res., Part A* **2015**, *103* (3), 949−958.

(42) Giles, C. H.; MacEwan, T. H.; Nakhwa, S. N.; Smith, D. 786. Studies in Adsorption. Part XI. A System of Classification of Solution Adsorption Isotherms, and Its Use in Diagnosis of Adsorption Mechanisms and in Measurement of Specific Surface Areas of Solids. *J. Chem. Soc.* **1960**, 3973−3993.

(43) Frey, S. T.; Guilmet, S. L.; Egan, R. G.; Bennett, A.; Soltau, S. R.; Holz, R. C. Immobilization of the Aminopeptidase from Aeromonas Proteolytica on Mg^{2+}/Al^{3+} Layered Double Hydroxide Particles. *ACS Appl. Mater. Interfaces* **2010**, *2*, 2828−2832.

(44) Vial, S.; Prevot, V.; Leroux, F.; Forano, C. Immobilization of Urease in ZnAl Layered Double Hydroxides by Soft Chemistry Routes. *Microporous Mesoporous Mater.* **2008**, *107*, 190−201.

(45) Cruz, J. C.; Pfromm, P. H.; Tomich, J. M.; Rezac, M. E. Conformational Changes and Catalytic Competency of Hydrolases Adsorbing on Fumed Silica Nanoparticles: I. Tertiary Structure. *Colloids Surf., B* **2010**, *79*, 97−104.

(46) Herrera, E.; Giacomelli, C. E. Surface Coverage Dictates the Surface Bio-Activity of D-Amino Acid Oxidase. *Colloids Surf., B* **2014**, *117*, 296−302.

(47) Geraud, E.; Prevot, V.; Forano, C.; Mousty, C. Spongy Gel-like Layered Double Hydroxide-Alkaline Phosphatase Nanohybrid as a Biosensing Material. *Chem. Commun. (Cambridge, U. K.)* **2008**, 1554−1556.

(48) Duy, C.; Fitter, J. How Aggregation and Conformational Scrambling of Unfolded States Govern Fluorescence Emission Spectra. *Biophys. J.* **2006**, *90*, 3704−3711.

(49) Kumari, A.; Rosenkranz, T.; Fitter, J.; Kayastha, A. M. Structural Stability of Soybean (Glycine Max) α-Amylase: Properties of the Unfolding Transition Studied with Fluorescence and CD Spectroscopy. *Protein Pept. Lett.* **2011**, *18*, 253−260.

(50) Lakowicz, J. R. *Principles of Fluorescence Spectroscopy*, 3rd ed.; Springer: Berlin, 2006.

(51) An, Z.; Lu, S.; He, J.; Wang, Y. Colloidal Assembly of Proteins with Delaminated Lamellas of Layered Metal Hydroxide. *Langmuir* **2009**, *25*, 10704−10710.

(52) Boclair, J. W.; Braterman, P. S. Layered Double Hydroxide Stability. 1. Relative Stabilities of Layered Double Hydroxides and Their Simple Counterparts. *Chem. Mater.* **1999**, *11*, 298−302.

(53) Parello, M. L.; Rojas, R.; Giacomelli, C. E. Dissolution Kinetics and Mechanism of Mg-Al Layered Double Hydroxides: A Simple Approach to Describe Drug Release in Acid Media. *J. Colloid Interface Sci.* **2010**, *351*, 134−139.

(54) Ambrogi, V.; Perioli, L.; Ciarnelli, V.; Nocchetti, M.; Rossi, C. Effect of Gliclazide Immobilization into Layered Double Hydroxide on Drug Release. *Eur. J. Pharm. Biopharm.* **2009**, *73*, 285−291.

(55) Bruna, F.; Pavlovic, I.; Celis, R.; Barriga, C.; Cornejo, J.; Ulibarri, M. A. Organohydrotalcites as Novel Supports for the Slow Release of the Herbicide Terbuthylazine. *Appl. Clay Sci.* **2008**, *42*, 194−200.

(56) Williams, G. R.; O'Hare, D. Towards Understanding, Control and Application of Layered Double Hydroxide Chemistry. *J. Mater. Chem.* **2006**, *16*, 3065.

(57) Rives, V.; del Arco, M.; Martín, C. Intercalation of Drugs in Layered Double Hydroxides and Their Controlled Release: A Review. *Appl. Clay Sci.* **2014**, *88−89*, 239−269.

(58) Zou, N.; Plank, J. Intercalation of Cellulase Enzyme into a Hydrotalcite Layer Structure. *J. Phys. Chem. Solids* **2015**, *76*, 34−39.